ME404: Numerical methods - buildings

The principle of superimposition, which underpins the response function method, has long been used by modellers to determine the response of a system to a set of excitations. This entails summing the responses, determined independently, of the system's component parts. If these parts are strongly interacting, as in the case of buildings and their environmental control systems, then this will lead to an inherent inaccuracy because the parts are decoupled. The practice of assuming model parameters (e.g. surface heat transfer coefficients, fabric conductivity etc. to be time invariant has the effect of decoupling parts and thereby rendering the principle of superimposition acceptable.

In the context of design tools intended to provide an early indication of performance trends, the response function and numerical modelling approaches are equally apt. Both can handle the dynamic interactions occurring within buildings, with the linearity and invariability assumptions of the former method being largely acceptable in terms of tool purpose. It is when this purpose changes to that of emulating reality that a clear distinction emerges. The response function method is a specific analytical technique, mathematically elegant and the outcome of many years of accumulated research and development. However, it is a technique which essentially emerged in response to the need to introduce dynamic considerations into manual methods. Numerical methods, on the other hand, evolved as a result of the dramatic inflation in computing power. The generality of these methods allow their direct application to the spectrum of target domains – building heat transfer, HVAC psychrometric processes, control, indoor air quality, electrical power flow, renewable energy conversion etc. – and, more significantly, to the integration of these domains.

Figure 1 summarises some of the domains that are candidates for coupling within a numerical simulation program. First order couplings include, but are not limited to, building thermal processes and natural illuminance distribution; building and plant thermal processes and distributed fluid flow; building thermal processes and intra-room air movement; building distributed air flow and intra-room air movement; electrical demand and micro power systems (renewable energy based or otherwise); and construction heat and moisture flow.

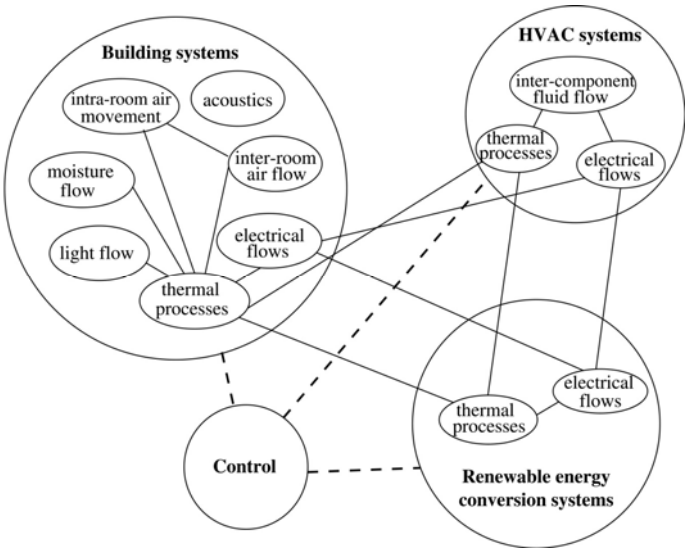

Figure 1: Examples of coupled technical domains.

Numerical methods are based on an approximation of some governing partial differential equation, such as the Fourier heat equation, which is applicable to regions where conduction prevails, or the Navier-Stokes momentum equation relating to fluid flow. This approximation is usually achieved by truncated Taylor series expansion or by application of conservation principles to small control volumes.

1. Equation formulation

Consider figure 2, which shows a continuous function f(γ) over the range between (γ-δγ) and (γ+δγ). The replacement of the derivatives of f(γ) by finite differences involves expressing these derivatives in terms of a truncated Taylor series expansion:

$$f(\gamma+\delta\gamma) = f(\gamma) + \delta\gamma f^{1}(\gamma) + \frac{(\delta\gamma)^2}{2} f^{2}(\gamma) + \frac{(\delta\gamma)^3}{6} f^{3}(\gamma) + \ldots$$

and

$$f(\gamma-\delta\gamma) = f(\gamma) - \delta\gamma f^{1}(\gamma) + \frac{(\delta\gamma)^2}{2} f^{2}(\gamma) - \frac{(\delta\gamma)^3}{6} f^{3}(\gamma) + \ldots$$

where $f^{n}(\gamma) = d^{n}f(\gamma)/d\gamma^{n}$.

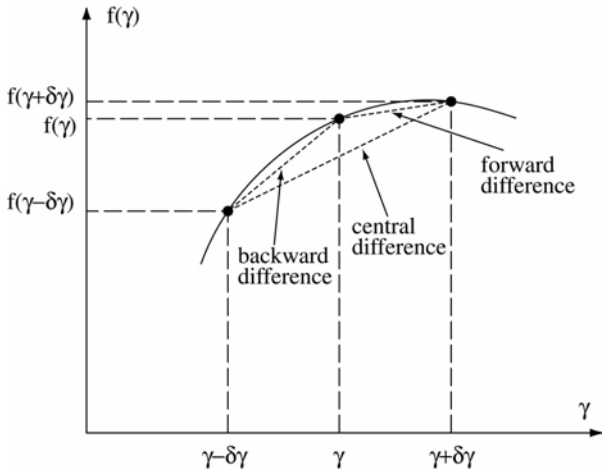

Figure 2: A continuous function of γ.

Adding these last two equations through those terms involving $(\delta\gamma)^3$ gives a central difference approximation for the second order derivative:

$$f^{2}(\gamma) = \frac{f(\gamma+\delta\gamma) - 2f(\gamma) + f(\gamma-\delta\gamma)}{(\delta\gamma)^2} + \varepsilon\left[(\delta\gamma)^2\right] \quad \ldots (1)$$

where $\varepsilon[(\delta\gamma)^2]$ indicates that the truncation error resulting from the approximate representation of the second order derivative is of order $(\delta\gamma)^2$; that is halving the discretisation step will approximately quarter the error.

Subtracting the second equation from the first through those terms involving δγ likewise gives a central difference approximation but for the first order derivative:

$$f^{1}(\gamma) = \frac{f(\gamma+\delta\gamma) - f(\gamma-\delta\gamma)}{2(\delta\gamma)} + \varepsilon\left[(\delta\gamma)^2\right] \quad \ldots (2)$$

Alternatively, truncating the first equation after the term involving δγ gives a first forward difference representation for the first order derivative:

$$f^{1}(\gamma) = \frac{f(\gamma+\delta\gamma) - f(\gamma)}{\delta\gamma} + \varepsilon[(\delta\gamma)] \quad \ldots (3)$$

while application of a similar truncation to the second equation gives a first backward difference representation:

$$f^{1}(\gamma) = \frac{f(\gamma) - f(\gamma-\delta\gamma)}{\delta\gamma} + \varepsilon[(\delta\gamma)] \quad \ldots (4)$$

Note that the truncation error associated with equations (3) and (4) is of order δγ, that is halving the discretisation step will only approximately half the error. Alternative mixes of equations (1) through (4) can be employed to give *explicit* and *implicit* difference formulations that enable the solution of systems governed by partial differential equations.

For example, figure 3 shows a homogeneous construction layer located within a multi-layered construction.

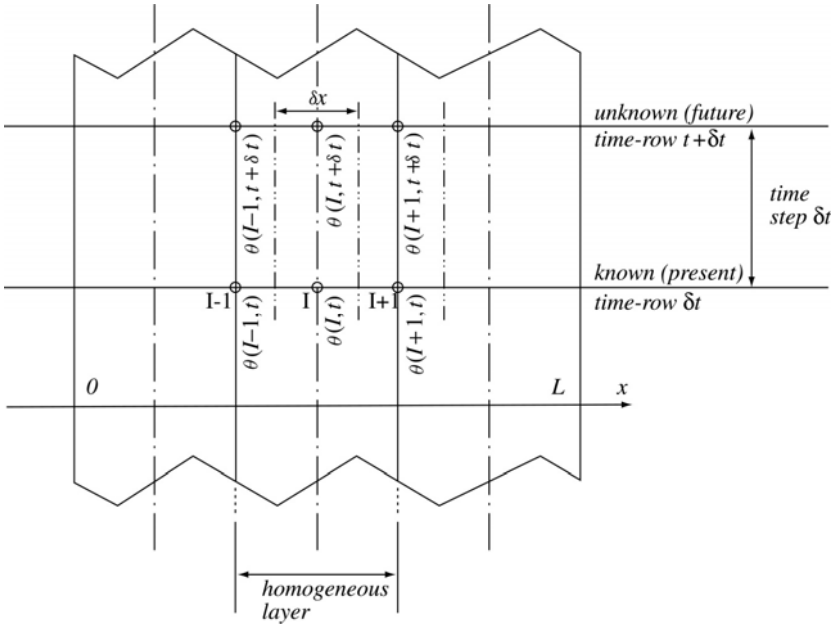

Figure 3: A homogeneous layer with space and time nodal scheme imposed.

The conduction of heat within such a system is governed by the Fourier equation, stated here in one space dimension and with heat generation:

$$\frac{\partial^2\theta(x,t)}{\partial x^2} = \frac{1}{\alpha}\frac{\partial\theta(x,t)}{\partial t} - \frac{q}{k} \quad \ldots (5)$$

An *explicit* scheme is obtained by replacing the second and first order derivatives in equation (5) by the central and first forward difference representations of equations (1) and (3) respectively. Ignoring the error term, this gives for node I at time t:

$$\frac{\theta(I+1,t)-2\theta(I,t)+\theta(I-1,t)}{(\delta x)^2} = \frac{1}{\alpha}\frac{\theta(I,t+\delta t)-\theta(I,t)}{\partial t} - \frac{q(I,t)}{k}$$

which, on rearrangement, gives

$$\theta(I+1,t+\delta t) = \frac{k\delta t}{\rho C(\delta x)^2}\theta(I+1,t) + \left(1-\frac{2k\delta t}{\rho C(\delta x)^2}\right)\theta(I,t) + \frac{k\delta t}{\rho C(\delta x)^2}\theta(I-1,t) + \frac{q(I,t)\delta t}{\rho C} \quad \ldots (6)$$

Note that the sum of the present time-row temperature term coefficients is unity implying that, in the absence of heat generation, the future time-row nodal temperature of any region I is a weighted average of the present time-row temperature in that region and the temperatures in adjacent regions, I+1 and I-1. If an equation of this form can be written for every region within a construction then, given initial and boundary conditions, the discrete temperature history over any required period can be determined. Explicit schemes of this type are relatively easy to formulate and solve but will become unstable if the coefficient of the present time-row temperature term of region I becomes negative, that is

$$1-\frac{2k\delta t}{\rho C(\delta x)^2} < 0$$

because this implies that the warmer region I is now, the colder it must be after a δt time step. To avoid this absurdity, a stability criterion is introduced:

$$\frac{2k\delta t}{\rho C(\delta x)^2} \le 1$$

more usually expressed as

$$F = \frac{\alpha\delta t}{(\delta x)^2} \le 1/2$$

where F is the Fourier number, defined as the ratio of the rate of heat conduction to heat storage. High values represent good conductors with relatively poor storage potential, while low values represent poor conductors with relatively good storage potential.

An *implicit* scheme is one in which the unknown temperature $\theta(I,t+\delta t)$ is expressed in terms of both the future and present time-row temperatures prevailing in all regions in thermal contact. Any given system will therefore be represented by a connected set of algebraic equations, which must be solved simultaneously at each simulation time-step. The second order derivative of equation (5) is replaced by the central difference formulation of equation (1) but using the unknown temperature values at the future time-row rather than the known values at the present time-row as in the explicit scheme. The first order derivative is expressed in the first backward formulation of equation (4). Ignoring the error term, this gives

$$\frac{\theta(I+1,t+\delta t)-2\theta(I,t+\delta t)+\theta(I-1,t+\delta t)}{(\delta x)^2}=\frac{1}{\alpha}\frac{\theta(I,t+\delta t)-\theta(I,t)}{\partial t}-\frac{q(I,t+\delta t)}{k}$$

which, on rearrangement, gives

$$\left(1+\frac{2k\delta t}{\rho C(\delta x)^2}\right)\theta(I,t+\delta t)=\theta(I,t)+\frac{k\delta t}{\rho C(\delta x)^2}\left[\theta(I+1,t+\delta t)+\theta(I-1,t+\delta t)\right]+\frac{q(I,t+\delta t)\delta t}{\rho C} \quad \ldots (7)$$

Implicit formulations are unconditionally stable for all space and time discretisation schemes although large space or time steps will result in excessive discretisation error. A weighted average of equations (6) and (7) gives rise to a numerical approximation to equation (5) that gives best accuracy and flexibility. This is done by multiplying equation (7) by a weighting factor, $0 \leq W \geq 1$, and adding the result to equation (6) after multiplication by (1-W):

$$(1+2WF)\theta(I,t+\delta t)=WF\left[\theta(I+1,t+\delta t)+\theta(I-1,t+\delta t)\right]+\left[1-2F(1-W)\right]\theta(I,t)$$
$$+(1-W)F\left[\theta(I+1,t)+\theta(I-1,t)\right]+\frac{\delta t}{\rho C}\left[Wq(I,t+\delta t)+(1-W)q(I,t)\right]$$

Setting $W \geq 0.5$ gives an implicit scheme, with W=0.5 resulting in the commonly used Crank-Nicolson formulation much favoured because of its stability combined with accuracy.

Differencing by Taylor series expansion is a formal way to establish a finite difference scheme from a known partial differential equation. Unfortunately the technique can be difficult to apply in all but simple problems. With energy systems typical complications include:

- the simultaneous presence of multiple heat transfer processes (conduction, convection, radiation, advection and heat generation);
- the time and positional dependency of heat generation due to solar radiation, mechanical plant etc.;
- the use of a discretisation method that leads to non-homogeneous, anisotropic finite volumes; and
- the presence of multi-dimensional effects.

An alternative approach is to directly apply conservation principles to small control volumes established to represent the physical system. This ensures that the resulting solution satisfies the conservation laws even if the number of control volumes is small (although in such a case discretisation errors might well dominate and/or the underlying physical models become badly represented).

Consider figure 4, which shows a control volume, I, communicating thermodynamically with four surrounding regions via the processes of conduction, convection, radiation and mass exchange (e.g. air and/or moisture flow). Internal heat generation is also considered to take place within the control volume (because of an electrical current or solar flux penetration for example).

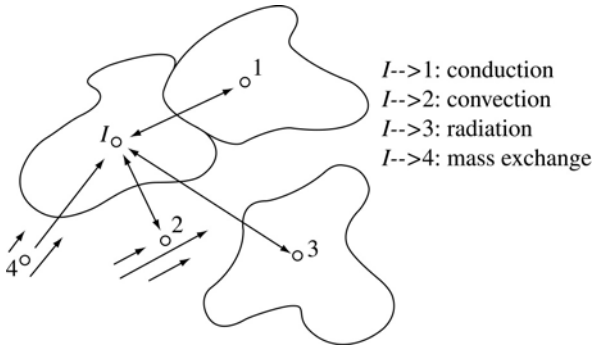

Figure 4: Energy exchanges in a physical system.

Assuming for the present purpose only that the inter-region heat exchange can be represented as a linear function of the temperature difference, each flow-path may be represented by

$$Q_{J,I} = K_{J,I}\left(\theta_J - \theta_I\right); J = 1,2,3,4 .$$

where $K_{J,I}$ is a heat flow conductance (W/°C).

The rate of heat storage within the region over some finite time interval, δt, is given by

$$Q_s = \frac{\rho_I(\xi)C_I(\xi)\delta V_I(\xi)}{\delta t}\left[\theta(I,t+\delta t)-\theta(I,t)\right]$$

where $\rho_I(\xi)$ is the density of region I at time ξ, $C_I(\xi)$ the specific heat capacity and $\delta V_I(\xi)$ the region volume.

Now, in the limit, the rate at which heat is being stored within I can be equated to the net rate of heat flow to the region and so, for the system of figure 4, heat balance considerations yield

$$\frac{\rho_I(\xi)C_I(\xi)\delta V_I(\xi)}{\delta t}\left[\theta(I,t+\delta t)-\theta(I,t)\right]=\left[\sum_{j=1}^{N} K_{j,I}\left(\theta_j-\theta_I\right)\_q_I\right]_{t=\xi} .$$

Evaluation of the heat flux and generation terms at the present time-row, ξ=t, gives the explicit formulation, while evaluation at the future time-row, ξ=t+δt, gives the fully implicit formulation. As above, an explicit/implicit mix can be obtained as a weighted summation of both schemes, which for a conduction problem becomes:

$$\begin{aligned} &C_s(t+\delta t)\theta(I,t+\delta t)-\sum_{i=1}^{N} C_{ci}(t+\delta t)\theta(i,t+\delta t)-\frac{\delta t q_I(t+\delta t)}{\delta V_I} \\ &=C_s(t)\theta(I,t)+\sum_{i=1}^{N} C_{ci}(t)\theta(i,t)+\frac{\delta t q_I(t)}{\delta V_I}+\varepsilon \end{aligned} \quad \ldots (8)$$

where $C_s(\xi)$ is the *self-coupling* coefficient at time ξ (=t or t+δt), $C_c(\xi)$ the *cross-coupling* coefficient, and N the number of inter-nodal contacts.

Most energy systems can be represented by three basis node types:

1. Nodes that represent the transient conduction within the materials comprising the building fabric, room contents and plant components.
2. Nodes that represent the energy balance at bounding surfaces such as indoor finishes, exposed roofs/walls and heat transfer interfaces within plant components.
3. Nodes that represent the energy balance within fluid volumes such as portions of room air or pipes and ducts.

Transient conduction

Figure 5 shows discrete regions, denoted I, I-1, I+1, J-1 etc., in conductive communication. Within this scheme, node I represents the discrete finite volume given by

$$(\delta_{I,I-1}+\delta_{I,I+1})\,(\delta_{I,J-1}+\delta_{I,J+1})\,(\delta_{I,K-1}+\delta_{I,K+1}).$$

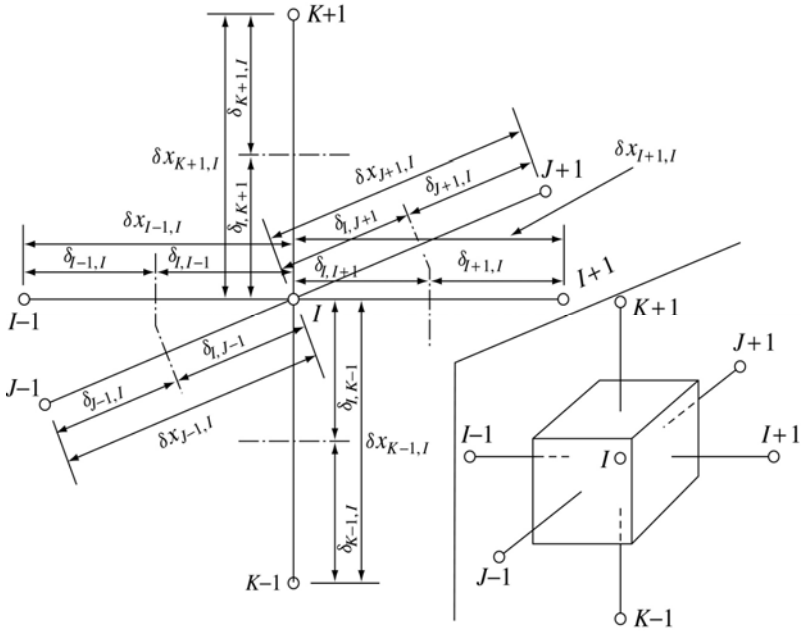

Figure 5: Transient conduction nodal scheme.

Application of equation (8) to such a case yields the unidirectional energy balance equation for an arbitrary placed node I:

$$\left[2\rho_I(t+\delta t)C_I(t+\delta t)+\frac{2\delta tk(t+\delta t)}{\delta x_I^2}\right]\theta(I,t+\delta t)-\frac{\delta tk(t+\delta t)}{\delta x_I^2}\theta(I+1,t+\delta t)-\frac{\delta tq_I(t+\delta t)}{\delta x_I\delta x_J\delta x_K}$$

$$=\left[2\rho_I(t)C_I(t)-\frac{2\delta tq_I(t+\delta t)}{\delta x_I^2}\right]\theta(I,t)+\frac{\delta tk(t)}{\delta x_I^2}\theta(I-1,t)+\frac{\delta tk(t)}{\delta x_I^2}\theta(I+1,t)+\frac{\delta tQ_I(t)}{\delta x_I\delta x_J\delta x_K}$$

Surface energy balance

Consider figure 6, which shows node I now located at some arbitrary surface. Node I-1 is the adjacent node buried within the material of the next-to-surface layer, J±1 and K±1 are the adjacent surface nodes, and I+1 the adjacent fluid volume.

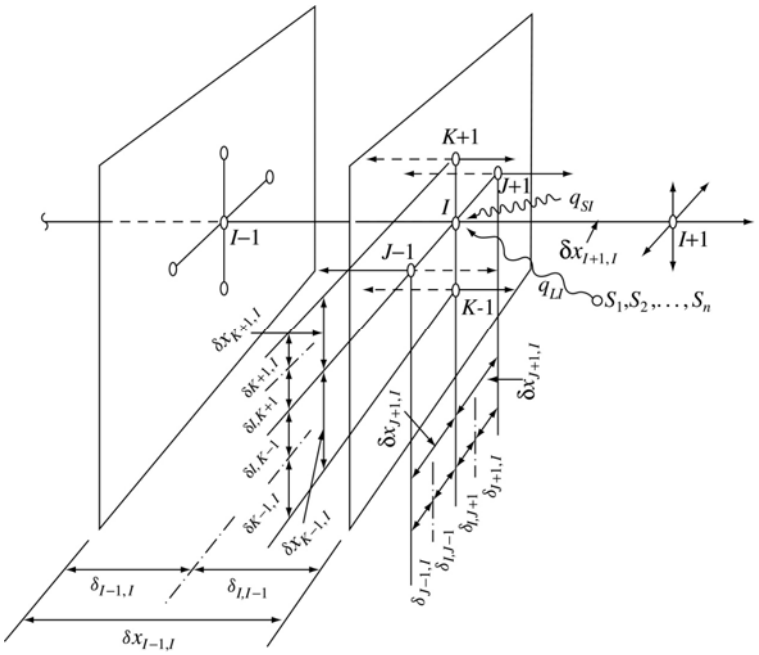

Figure 6: Surface energy balance nodal scheme.

The unidirectional heat balance equation for this case is given by

$$\left[2W_I(t+\delta t)+\frac{\delta t k'_{I-1,I}(t+\delta t)}{\delta x_{I-1,I}\delta_{I-1,I}}+\frac{\delta t h_{cI+1,I}(t+\delta t)}{\delta_{I,I-1}}+\frac{\delta t\sum_{s=1}^{N}h_{rs,I}(t+\delta t)}{\delta_{I,I-1}}\right]\theta(I,t+\delta t)-\frac{\delta t k'_{I-1,I}(t+\delta t)}{\delta x_{I-1,I}\delta_{I,I-1}}\theta(I-1,t+\delta t)$$

$$-\frac{\delta t h_{cI+1,I}(t+\delta t)}{\delta_{I,I-1}}\theta(I+1,t+\delta t)-\frac{\delta t\sum_{s=1}^{N}h_{rs,I}(t+\delta t)\theta(s,t+\delta t)}{\delta_{I,I-1}}-\frac{\delta t q_{PI}(t+\delta t)}{\delta_{I,I-1}\delta_{J-1,J+1}\delta_{K-1,K+1}}$$

$$=\left[2W_I(t)-\frac{\delta t k'_{I-1,I}(t)}{\delta x_{I-1},I\delta_{I,I-1}}-\frac{\delta t h_{cI+1,I}(t)}{\delta_{I,I-1}}-\frac{\delta t\sum_{s=1}^{N}h_{rs,I}(t)}{\delta_{I,I-1}}\right]\theta(I,t)+\frac{\delta t k'_{I-1,I}(t)}{\delta x_{I-1,I}\delta_{I,I-1}}\theta(I-1,t)+\frac{\delta t h_{cI+1,I}(t)}{\delta_{I,I-1}}\theta(I+1,t)$$

$$+\frac{\delta t\sum_{s=1}^{N}h_{rs,I}(t)\theta(s,t)}{\delta_{I,I-1}}+\frac{\delta t\left[q_{PI}(t)+q_{SI}(t)+q_{RI}(t)+q_{SI}(t+\delta t)+q_{RI}(t+\delta t)\right]}{\delta_{I,I-1}\delta_{J-1,J+1}\delta_{K-1,K+1}}+\varepsilon.$$

Fluid volumes

Figure 7 shows the case where node I is located at the centroid of some fluid volume bounded by a collection of fictitious and/or real faces comprising the interfaces with adjacent fluid volumes, exposed surface layers, ambient conditions, plant components etc.

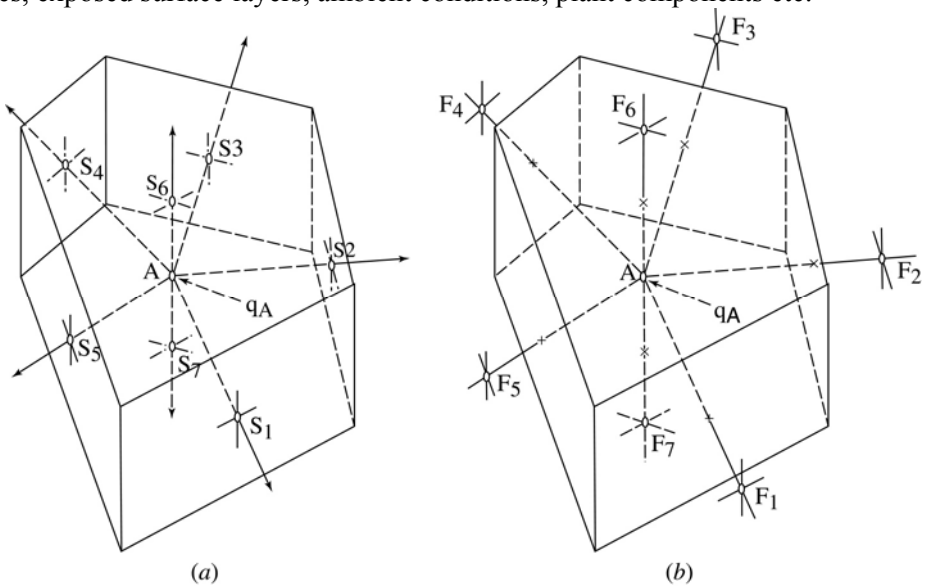

Figure 7: Fluid volume energy balance nodal scheme:
(a) fluid contained by real surfaces; convective heat transfer
(b) fluid contained by fictitious surfaces; advective heat transfer.

The unidirectional heat balance equation for this case is given by

$$\left[2W_I(t+\delta t)+\frac{\delta t\sum_{i=1}^{N}h_{ci,I}(t+\delta t)\delta A_{i,I}}{\delta V_I}+\frac{\delta t\sum_{j=1}^{M}v_{j,I}(t+\delta t)\rho_{j,I}(t+\delta t)C_{j,I}(t+\delta t)}{\delta V_I}\right]\theta(I,t+\delta t)$$

$$-\frac{\delta t\sum_{i=1}^{N}h_{ci,I}(t+\delta t)A_{i,I}\theta(i,t+\delta t)}{\delta V_I}-\frac{\delta t\sum_{j=1}^{M}v_{j,I}(t+\delta t)\rho_{j,I}(t+\delta t)C_{j,I}(t+\delta t)\theta(j,t+\delta t)}{\delta V_I}-\frac{\delta tq_{PI}(t+\delta t)}{\delta V_I}$$

$$=\left[2W_I(t)-\frac{\delta t\sum_{i=1}^{N}h_{ci,I}(t)\delta A_{i,I}}{\delta V_I}-\frac{\delta t\sum_{j=1}^{M}v_{j,I}(t)\rho_{j,I}(t)C_{j,I}(t)}{\delta V_I}\right]\theta(I,t)+\frac{\delta t\sum_{i=1}^{N}h_{ci,I}(t)\delta A_{i,I}\theta(i,t)}{\delta V_I}$$

$$+\frac{\delta t\sum_{j=1}^{M}v_{j,I}(t)\rho_{j,I}(t)C_{j,I}(t)\theta(j,t)}{\delta V_I}+\frac{\delta tq_I(t)}{\delta V_I}+\varepsilon.$$

2. Formulating the overall system equations

The formulation of a complete numerical model is essentially a three stage process as follows.

1. The energy system is made discrete by the placement of 'nodes' at points of interest. These nodes represent homogeneous or non-homogeneous physical volumes corresponding to room air, opaque and transparent boundary surfaces, constructional elements, plant component parts, renewable energy components and so on.
2. For each node in turn, and in terms of all other nodes representing regions deemed to be in thermodynamic contact, conservation equations of the above form are developed to represent the nodal condition and the inter-nodal transfers of energy, mass and momentum.
3. The entire equation-set is solved simultaneously for successive time steps to obtain the future time-row nodal state variables as a function of the present time-row states and prevailing boundary conditions at both time-rows.

There are two main types of error associated with finite differencing schemes: rounding errors and discretisation errors. The former occur in cases where computations include an insufficient number of significant figures. Any tendency towards an accumulation of such errors can rapidly become critical, especially in large numerical schemes involving many computational operations. Fortunately, errors of this type can be reduced to insignificance by the careful design of the numerical scheme and by operating, where appropriate, in double precision.

Discretisation errors result from the replacement of derivatives by finite differences. Although unavoidable, such errors can usually be minimised by reducing the space and time increments. Whilst accuracy considerations dictate that such increments be small, considerations of computational speed require that they be made relatively large. Although it is impossible to predetermine the space and time increments for a given accuracy level, optimum values can be ascertained from simple parametric studies using the developed model. This implies that a model must first be developed against the assumption that any increment is possible. This greatly promotes the use of implicit formulations because they are unconditionally stable and, if well designed, consistent with the original partial differential equation-set.

In schemes involving more than one space dimension it is not possible to prescribe the nodal placements since this will depend on such factors as internal and external surface insolation, the existence of localised convection, the presence of corner effects and thermal bridges, and the shape of the capacity/insulation system being modelled: all factors causing position dependent transient effects. Nevertheless, in many applications n-dimensional schemes will become necessary, with mixed-dimensional schemes proving useful. Figure 8, for example, gives some example mixed schemes and their corresponding application.

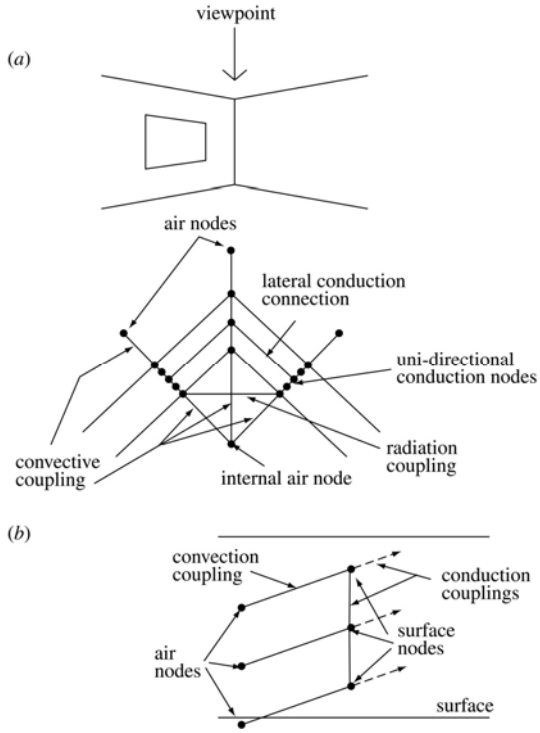

Figure 8: Some mixed nodal schemes and their typical applications:
(a) corner effects – a combined one- and two-dimensional scheme;
(b) surface temperature gradient – a two-dimensional scheme.

Likewise, it is not possible to prescribe the spatial subdivision of fluid volumes (room air, boiler combustion chamber, wall cavity etc.) although a number of general points can be made. It is usually desirable to subdivide the volume vertically to include the buoyancy effects of density variations resulting in stratification. Local, fine discretisation will be required adjacent to bounding surfaces – to allow the effects of solar patch movement to be studied or to support a link between the building fabric and an adjacent computational fluid dynamics domain. Global, fine discretisation will be required where intra-space air movement, comfort distribution and indoor air quality are the issues to be studied. In general terms, the subdivision criteria will depend on the expected variations of fundamental thermo-physical properties and heat fluxes throughout the system, on the extent to which distinct regions will be subjected to control action, and the ultimate simulation objectives.

Equation structuring

Utilising the above formulations it is possible to construct a mathematical model of a real scale problem. The procedure involves devising a suitable discretisation scheme, generating the corresponding conservation equations, and arranging for equation-set solution when parts of the problem are constrained by control action.

This section demonstrates equation structuring by presenting some example problems that demonstrate the form of the overall matrix equation to result.

Figure 9 shows a single zone comprising 6 multi-layered constructions, 6 surface layers and 2 fluid volumes. A rudimentary nodal scheme is imposed to represent uni-directional transient conduction, surface exchanges and the exchange of air between lower and upper portion. The entire system is represented by 50 nodes and so there will be 50 simultaneous equations each comprising one self- and several cross-coupling coefficients relating to the present and future time-rows of the computational time steps throughout the simulation period..

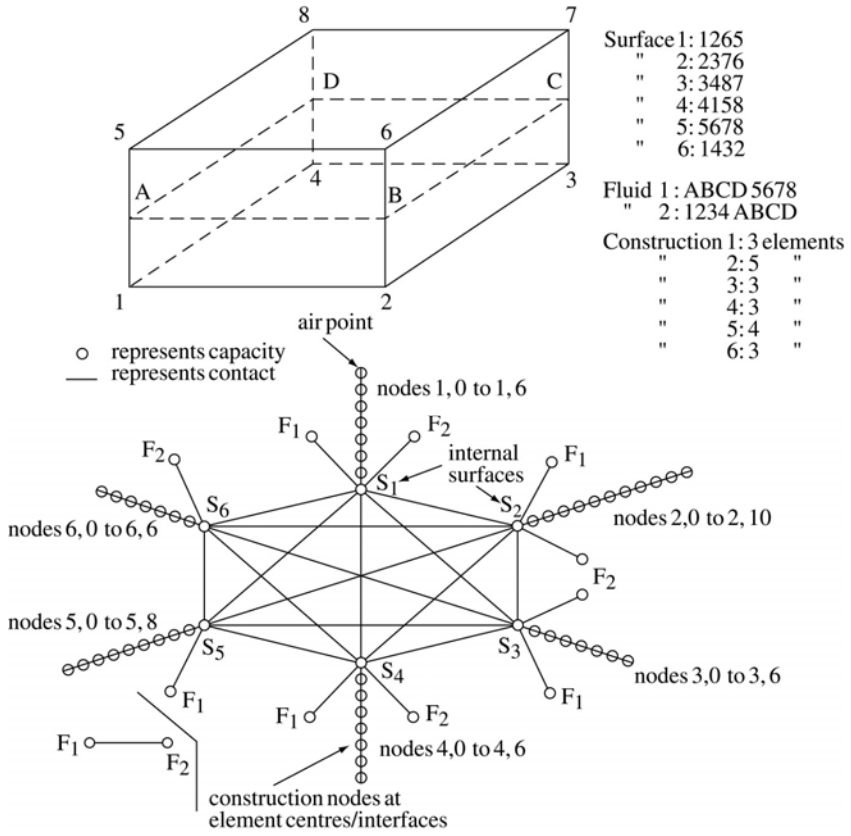

Figure 9: A single zone system and equivalent nodal scheme.

Figure 10 shows the form of the **A** coefficients matrix of the overall equation-set:

$$\mathbf{A}.\boldsymbol{\theta}_{n+1} = \mathbf{B}.\boldsymbol{\theta}_n + \mathbf{C} \quad \ldots (9)$$

The **A** matrix is not square since coefficients relating to future time-row boundary nodes are retained on the left-hand side (future time-row) of each equation even though, in any given problem, their numerical value is known. This is necessary to allow matrix interlocking when other components or building zones are added to effectively remove the problem boundary elsewhere. Even when boundary condition terms are removed to the equation right-hand side, the **A** matrix will remain non-square for all systems in which some nodal heat injection/extraction is to be determined as a function of user-specified control constraints. The solution of the above equation-set can then be achieved by the inclusion of negative feedback or feed-forward control action. Alternatively, the coefficient entry relating to the heat interaction terms can be replaced by a plant matrix equation which is interlocked with the various building zones.

The two-dimensional arrays **A** and **B** have the same number of rows as system equations and any existing element a_{ij} or b_{ij} ($i \neq j+1$) is a coefficient which links two nodal regions at the future and present time-rows respectively of the time step for which the matrix was established. Any zero valued element indicates that no coupling exists between the nodal regions in question. Elements a_{ii+1} and b_{ii+1} are self-coupling coefficients, which represent the storage potential of the region represented by equation i. The column matrices $\boldsymbol{\theta}_{n+1}$ and $\boldsymbol{\theta}_n$

contain the nodal temperature terms and heat injection/extractions at the future and present time-rows respectively. The column matrix **C** contains the known boundary condition excitations due to the temperature and heat flux fluctuations that act on selected nodes to cause energy flow and so `drive' a simulation.

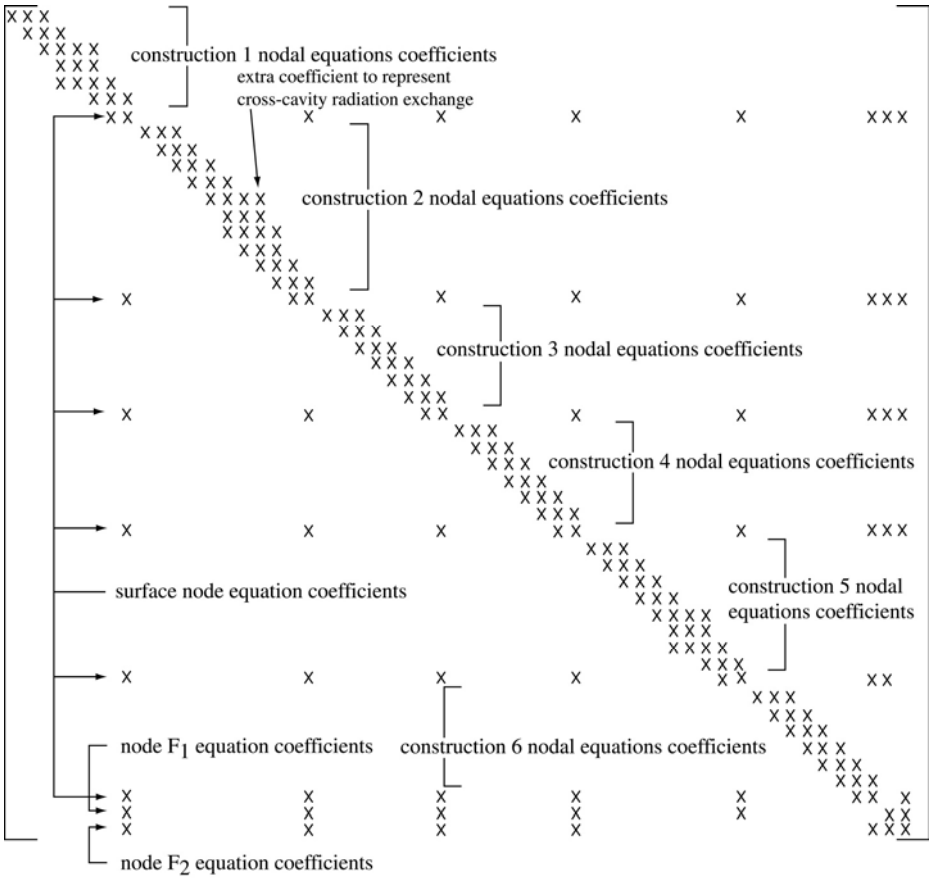

Figure 10: The future time-row coefficients matrix **A** of the single zone matrix equation $\mathbf{A}.\boldsymbol{\theta}_{n+1} = \mathbf{B}.\boldsymbol{\theta}_n + \mathbf{C}$.

Since all terms on the right-hand side of equation (9) relate either to the known present time-row (**B** and $\boldsymbol{\theta}_n$) or are known boundary terms (**C**), it is appropriate to generate a column matrix **Z** where $\mathbf{Z} = \mathbf{B}_n + \mathbf{C}$. Equation (9) can then be re-expressed as

$$\mathbf{A}.\boldsymbol{\theta}_{n+1} = \mathbf{Z}$$

and the solution by

$$\boldsymbol{\theta}_{n+1} = \mathbf{A}^{-1}.\mathbf{Z}.$$

Various techniques exist to achieve this solution with the outputs supporting an assessment of energy and comfort, and providing details on the contribution of issues such as infiltration & ventilation, short- & longwave radiation, casual gains and so on. Such outputs would not support the study of localised convective phenomena, thermal bridging, indoor air quality or the assessment of plant performance to predict energy consumption. For this purpose the nodal network must be extended.

Figure 11 shows several single zones combined to form a small multi-zone system with a central boiler and distributed radiator system superimposed. Again, transient conduction is

uni-directional (for clarity) but in one zone a multi-directional scheme has been incorporated to facilitate the study of corner effects and thermal bridges. A simple nodal scheme is used to represent distribution losses, with a more detailed scheme applied to the various boiler sections.

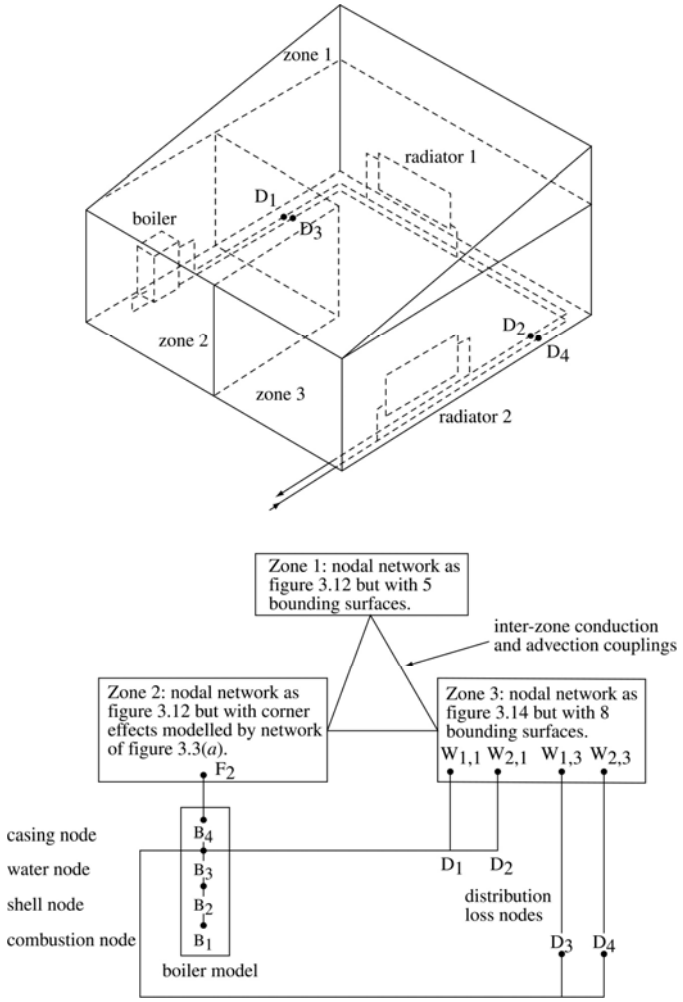

Figure 11: A multi-zone building with boiler and distributed radiator scheme.

Figure 12 gives the equivalent equation system. This model will allow, in addition to the analysis potential of the previous example, a detailed investigation of the energy and comfort related aspects of building performance: building and plant zoning strategies, global versus zone level control, whole building energy requirements and consumption, boiler efficiency studies, distribution losses, priority and optimum start control regimes, to name but a few.

3. Solving the system equations

Because the system of equations contain both present and future time-row terms, they must be solved simultaneously. And because the entire system is sparse and populated by clusters of equations relating to components with different time constants, a specially adapted solver will be required to minimise the computational effort.

There are two main solution techniques: iterative and direct. In general terms, direct methods require more storage space than do iterative methods and may prove inefficient when applied to large, sparse equation systems as is the case here. However, direct methods may be used as the building block of an efficient solver for sparse equation systems where different equation clusters are processed at a different frequency depending on the time constant of the corresponding physical system. This allows control decisions to be made, and thermo-

physical properties recomputed, more frequently for an item of plant requiring a computational time-step of, say, 1 minute, than for a heavyweight construction requiring, say, 60 minutes. Such an approach to solution ensures that only the actual physical scheme is addressed by partitioning the overall (and sparse) system matrix into a number of discrete sub-matrices so that solution can be achieved in the lowest number of computational steps (because the capabilities and features of simulation programs are constantly evolving, computation times are still problematic despite advances in processor technology). Each partitioned matrix can then be processed as far as possible by a direct method, and at any frequency, with the inter-component information brought together to permit the global solution stream to continue. As circumstances allow, any sub-matrix need not be reprocessed until its contents (the equation coefficients) have changed by an appreciable amount.

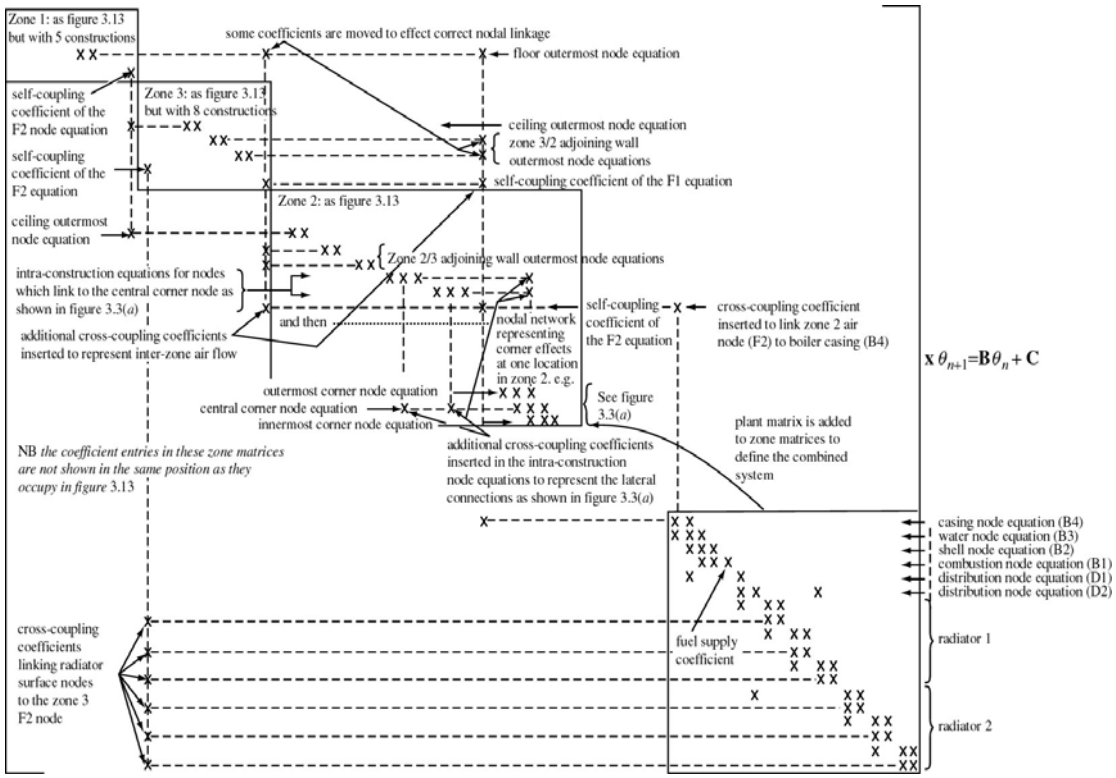

Figure 12: The energy balance matrix equation for the system of figure 11.